

Chalcogenide Chemistry in Ionic Liquids: Nonlinear Optical Wave-Mixing Properties of the Double-Cubane Compound $[\text{Sb}_7\text{S}_8\text{Br}_2](\text{AlCl}_4)_3$

Qichun Zhang,[†] In Chung,[†] Joon I. Jang,[‡] John B. Ketterson,[‡] and Mercuri G. Kanatzidis^{*,†,§}

Department of Chemistry and Department of Physics and Astronomy, Northwestern University, Evanston, Illinois 60208, and Materials Science Division, Argonne National Laboratory, Chicago, Illinois 60439

Received May 13, 2009; E-mail: m-kanatzidis@northwestern.edu

Ionic liquids as “supersolvents” are now recognized as powerful reaction media for preparing functional materials such as zeolites,¹ metal–organic frameworks,¹ metal nanoparticles,² and organic compounds³ as well as being useful in separations,⁴ electrochemistry,⁵ and nanotechnology.⁶ Ionic liquids are in fact special molten salts and have high thermal stability, high ionic conductivity, a broad liquid-state temperature range, low vapor pressure, and the ability to dissolve a variety of materials. They tend to contain large organic cations with high polarizability. These features make them unique media in materials science.⁶

The synthesis of chalcogenides in molten salts is a well-established approach,⁷ but it has been less-explored in ionic liquids containing organic cations. Chalcogenides have not only diverse structures but also technologically promising properties such as thermoelectric and solar energy conversion,⁸ phase-change transitions,⁹ photocatalysis,¹⁰ ionic conductivity,¹¹ and ion exchange.¹² Ionic liquids could offer fascinating possibilities for producing new structures in chalcogenides and unprecedented properties.

Although the preparation of binary chalcogenide nanoparticles in ionic liquids has been reported,¹³ the synthesis of new chalcogenides is still in its infancy. Here we demonstrate the use of the ionic liquid EMIMBr–AlCl₃ (EMIM = 1-ethyl-3-methylimidazolium) as a solvent in the preparation of a new material featuring a cationic chalcogenide. This is the first time that cationic chalcogenide clusters have been synthesized in ionic liquids. Prior to this work, the only chalcogenide materials prepared in ionic liquids were the anionic frameworks (PhP₄)[M(Se₆)₂] (M = Ga, In, Tl), which were reported in 1992.¹⁴

Chalcogenide polycationic clusters are a very interesting subgroup with various structures.¹⁵ They can be synthesized in electrophilic and acidic media such as liquid SO₂ and H₂SO₄, or using strong oxidizing agents such as WCl₅,¹⁶ SbF₅, and AsF₅,¹⁷ or in the presence of strong acceptors such as AlCl₃¹⁸ and ZrCl₄.¹⁹ We show here that chalcogenide polycationic clusters can be conveniently synthesized in ionic-liquid media containing Lewis acids or strong acceptors.

The new compound $[\text{Sb}_7\text{S}_8\text{Br}_2](\text{AlCl}_4)_3$ (**1**) was synthesized in 42% yield by reacting Sb with S in EMIMBr–AlCl₃ ionic liquid (1:11 EMIMBr/AlCl₃ molar ratio) at 165 °C for 10 days. The red crystals of **1** exhibit nonlinear optical (NLO) properties, including difference-frequency generation (DFG) and second harmonic generation (SHG). The structure of compound **1** was determined from single-crystal X-ray diffraction data collected at 100 K on a STOE 2T X-ray diffractometer.

Compound **1** crystallizes in the noncentrosymmetric space group $P2_12_12_1$.²⁰ The crystal structure of **1** consists of cationic $[\text{Sb}_7\text{S}_8\text{Br}_2]^{3+}$

clusters and $[\text{AlCl}_4]^-$ anions (Figure 1). Each cluster adopts a unique double-cubane structure in which two distorted cubic clusters connect by sharing one corner (the Sb1 site). The other corners are alternately occupied with Sb and S atoms. Two Sb sites (Sb2 and Sb6) have terminal Sb–Br bonds projecting out of the cluster structure.

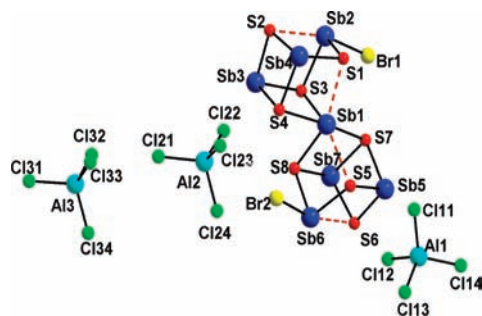


Figure 1. Structure of the compound $[\text{Sb}_7\text{S}_8\text{Br}_2](\text{AlCl}_4)_3$ (**1**). Color code: blue, Sb; red, S; yellow, Br; cyan, Al; green, Cl. The red dashed lines show weak Sb–S bonds (2.938–3.136 Å).

The cationic $[\text{Sb}_7\text{S}_8\text{Br}_2]^{3+}$ clusters pack in pseudohexagonally arranged columns along the crystallographic *a* axis and display a pronounced hexagonal pseudosymmetry (Figure 2). The voids between the cationic clusters are filled with $[\text{AlCl}_4]^-$ anions, and each cationic cluster is surrounded by eight $[\text{AlCl}_4]^-$ anions. All of the crystallographically independent $[\text{AlCl}_4]^-$ ions adopt a slightly distorted tetrahedral shape (Figure 2). The Al–Cl bond lengths range from 2.093(4) to 2.167(3) Å and the Cl–Al–Cl angles from 106.22(14) to 112.73(15)°.

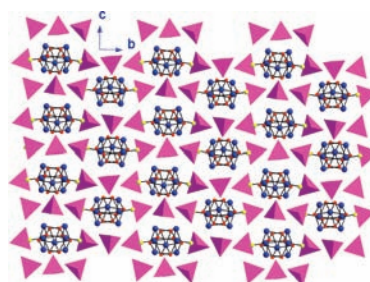


Figure 2. Stacking view of the ions in compound **1** along the *a* axis. Blue balls, Sb atoms; red balls, S atoms; yellow balls, Br atoms; purple tetrahedra, $[\text{AlCl}_4]^-$ anions.

It is worth noting that there are three different geometries in the Sb sites of the cubes. The corner-shared Sb1 center has an unusual sixfold coordination, with S–Sb–S angles ranging from 78.14(5) to 166.3(1)°. Two short Sb–S bonds {Sb1–S3 [2.599(2) Å] and Sb1–S8 [2.628(2) Å]},²¹ two intermediate ones {Sb1–S4 [2.695(2)

[†] Department of Chemistry, Northwestern University.

[‡] Department of Physics and Astronomy, Northwestern University.

[§] Argonne National Laboratory.

Å) and Sb1–S7 [2.747(2) Å]), and two long ones {Sb1–S1 [2.948(3) Å] and Sb1–S5 [2.996(3) Å]} to the Sb1 center can be clearly observed. The Sb2 and Sb6 atoms are fourfold-coordinated by three sulfur atoms and one bromide atom to form seesaw-shaped geometries, where two weak Sb–S bonds {Sb2–S2 [3.135(3) Å] and Sb6–S6 [3.136(4) Å]} are observed. The remaining Sb centers (Sb3, Sb4, Sb5, and Sb7) are trigonal-pyramidally coordinated by three sulfur atoms.

Optical absorption spectroscopy of single crystals of **1** revealed absorption edges at ~ 2.03 eV, consistent with the red color (Figure 3a). Presumably, this originates from an electronic transition associated with the $[\text{Sb}_7\text{S}_8\text{Br}_2]^{3+}$ clusters. Thermogravimetric analysis (TGA) under N_2 atmosphere (Figure S3 in the Supporting Information) showed that compound **1** starts to lose weight at a low temperature (350 K) and undergoes a sharp weight loss at 550 K, leaving a residue that is a mixture of Al_2O_3 , Sb_2S_3 , and $\text{SbSBr}_{1-x}\text{Cl}_x$, the last of which is amorphous (Figure S4). Therefore, the weight loss is attributed to AlCl_3 and $\text{AlCl}_{3-x}\text{Br}_x$ species.

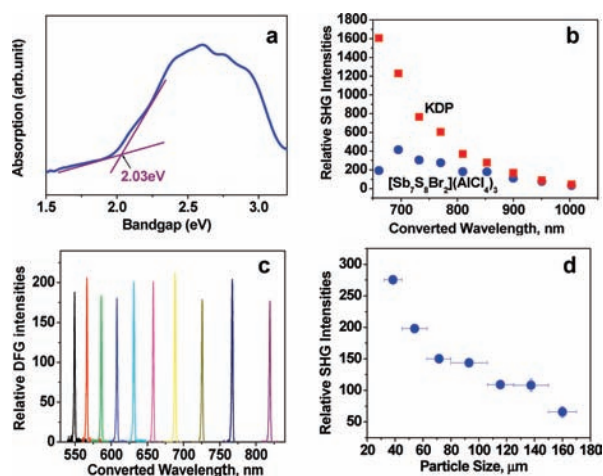


Figure 3. (a) Electronic absorption spectrum of a single crystal of **1**. (b) SHG intensity (arbitrary units) of **1** (blue) relative to KDP (red). (c) DFG vs wavelength accomplished with polycrystalline **1**. (d) Particle-size dependence of the SHG intensity generated from polycrystalline **1**.

Because of the wide optical transparency region (3.57–7.81 μm) and noncentrosymmetric structure of compound **1** (Figure S5), we investigated its NLO SHG response using a modified Kurtz powder method.²² The SHG intensities generated by compound **1** were directly compared with those of KH_2PO_4 (KDP) powder. KDP is a benchmark NLO material that is transparent from 0.22 to 1.1 μm , and its SHG susceptibility is $\chi_{\text{eff}}^{(2)} = 1.0$ pm/V.²³ SHG intensities of samples prepared in a similar fashion and having the same particle size range (45.5 ± 7.5 μm) as KDP were measured and compared with those for KDP. The SHG intensity of compound **1** is approximately one-third that of KDP at 700 nm and becomes comparable to that of KDP above 900 nm (Figure 3b). Compound **1** produced second-harmonic light in the visible and near-IR region upon sweeping the fundamental wavelength.

In order to test the wave-mixing capability of compound **1**, we performed DFG experiments, which are essential for generating mid-IR light and facilitating multichannel conversion. Both the idler (λ_1) and signal (λ_2) beams were generated by an optical parametric amplifier driven by a pulsed Nd:YAG laser at 355 nm. From the energy conservation law [$1/\lambda_1 + 1/\lambda_2 = 1/(355 \text{ nm})$] and the definition of DFG ($1/\lambda_2 - 1/\lambda_1 = 1/\lambda_{\text{DFG}}$), the expected wavelength for DFG for a given λ_1 is determined as $\lambda_{\text{DFG}} = [\lambda_1/(\lambda_1 - 710 \text{ nm})] \times 355 \text{ nm}$.

Through the use of different combinations of λ_1 and λ_2 , compound **1** successfully generated continuously tunable visible and near-IR light by DFG (Figure 3c). Deviations among the DFG intensities arose from the signal beam when the energy was above the band gap. Although our detection limit (< 1 μm) prohibited the observation of DFG in the mid-IR, the compound should produce tunable coherent light throughout the mid-IR because it is optically transparent in this region, for which few NLO materials are available.^{24,25} $[\text{Sb}_7\text{S}_8\text{Br}_2](\text{AlCl}_4)_3$ is type-I non-phase-matchable because the SHG intensities decrease with increasing particle size (Figure 3d), but it can be still useful with “random” quasi-phase-matching.²⁶

The ability to stabilize Lewis acids in organic ionic liquids creates new synthetic opportunities for discovering metal chalcogenides with cationic character rather than the typical anionic nature observed to date in molten salt chemistry.

Acknowledgment. Financial support from the National Science Foundation (DMR-0801855) is gratefully acknowledged.

Supporting Information Available: An SEM image, powder XRD, EDS, IR, and TGA analysis data, and an X-ray crystallographic file (CIF) for compound **1**. This material is available free of charge via the Internet at <http://pubs.acs.org>.

References

- (1) Morris, R. E. *Angew. Chem., Int. Ed.* **2008**, *47*, 442.
- (2) (a) Migowski, P.; Dupont, J. *Chem.—Eur. J.* **2007**, *13*, 32. (b) Guloy, A. M.; Ramlau, R.; Tang, Z.; Schnelle, W.; Baitinger, M.; Grin, Y. *Nature* **2006**, *443*, 320.
- (3) (a) Aumann, M.; Riisager, A. *Chem. Rev.* **2008**, *108*, 1474. (b) Tundo, P.; Perosa, A. *Chem. Soc. Rev.* **2007**, *36*, 532.
- (4) Han, X.; Armstrong, D. W. *Acc. Chem. Res.* **2007**, *40*, 1079.
- (5) El Abedin, S. Z.; Endres, F. *Acc. Chem. Res.* **2007**, *40*, 1106.
- (6) Lodge, T. P. *Science* **2008**, *321*, 50.
- (7) (a) McCarthy, T. J.; Kanatzidis, M. G. *Inorg. Chem.* **1995**, *34*, 1257. (b) Chondroudis, K.; McCarthy, T. J.; Kanatzidis, M. G. *Inorg. Chem.* **1996**, *35*, 840.
- (8) Hsu, K. F.; Loo, S.; Guo, F.; Chen, W.; Dyck, J. S.; Uher, C.; Hogan, T.; Polychroniadis, E. K.; Kanatzidis, M. G. *Science* **2004**, *303*, 818.
- (9) (a) Yu, D.; Brittan, S.; Lee, J. S.; Falk, A. L.; Park, H. *Nano Lett.* **2008**, *8*, 3429. (b) Lee, J. S.; Brittan, S.; Yu, D.; Park, H. *J. Am. Chem. Soc.* **2008**, *130*, 6252.
- (10) Zheng, N.; Bu, X.; Vu, H.; Feng, P. *Angew. Chem., Int. Ed.* **2005**, *44*, 5299.
- (11) Feng, P.; Bu, X.; Zheng, N. *Acc. Chem. Res.* **2005**, *38*, 293.
- (12) (a) Manos, M. J.; Ding, N.; Kanatzidis, M. G. *Proc. Natl. Acad. Sci. U.S.A.* **2008**, *105*, 10. (b) Poudeu, P. F. P.; D’Angelo, J.; Downey, A. D.; Short, J. L.; Hogan, T. P.; Kanatzidis, M. G. *Angew. Chem., Int. Ed.* **2006**, *45*, 3835.
- (13) (a) Biswas, K.; Rao, C. N. R. *Chem.—Eur. J.* **2007**, *13*, 6123. (b) Jiang, Y.; Zhu, Y. J. *J. Phys. Chem. B* **2005**, *109*, 4361.
- (14) Dhingra, S.; Kanatzidis, M. G. *Science* **1992**, *258*, 1796.
- (15) Brownridge, S.; Krossing, I.; Passmore, J.; Jenkins, H. D. B.; Roobottom, H. K. *Coord. Chem. Rev.* **2000**, *197*, 397.
- (16) Beck, J.; Wetterau, J. *Inorg. Chem.* **1995**, *34*, 6202.
- (17) Klapötke, T.; Passmore, J. *Acc. Chem. Res.* **1989**, *22*, 234.
- (18) Beck, J.; Dolg, M.; Schlüter, S. *Angew. Chem., Int. Ed.* **2001**, *40*, 2287.
- (19) Beck, J.; Hedderich, S. *J. Solid State Chem.* **2003**, *172*, 12.
- (20) Single-crystal X-ray diffraction data were collected at 100 K using a STOE 2T imaging-plate diffraction system with graphite-monochromatized Mo K α radiation. A numerical and empirical absorption correction was applied. Direct methods and full-matrix least-squares refinements against F^2 were performed with the *SHELXTL* package. Crystal data for $[\text{Sb}_7\text{S}_8\text{Br}_2](\text{AlCl}_4)_3$ (**1**): orthorhombic; $P2_12_12_1$; $Z = 4$; $a = 11.989(2)$ Å, $b = 16.896(3)$ Å, $c = 17.378(4)$ Å; $V = 3520.2(12)$ Å³. Collection and refinement data: $T = 100$ K; $2\theta_{\text{max}}(\text{Mo K}\alpha) = 53.52^\circ$; $D_{\text{calc}} = 3.349$ g/cm³; $F(000) = 3192$; 7431 total reflections; 7004 unique reflections [$F_o^2 > 2\sigma(F_o^2)$]; 289 parameters; GOF = 1.126; $R1 = 3.61\%$ and $wR2 = 8.47\%$ for $I > 2\sigma(I)$.
- (21) Ding, N.; Kanatzidis, M. G. *Chem. Mater.* **2007**, *19*, 3867.
- (22) Kurtz, S. K.; Perry, T. T. *J. Appl. Phys.* **1968**, *39*, 3798.
- (23) Dunn, M. H.; Ebrahimzadeh, M. *Science* **1999**, *286*, 1513.
- (24) Fiore, A.; Berger, V.; Rosencher, E.; Bravetti, P.; Nagle, J. *Nature* **1998**, *391*, 463.
- (25) Bera, T. K.; Jang, J. I.; Ketterson, J. B.; Kanatzidis, M. G. *J. Am. Chem. Soc.* **2009**, *131*, 75.
- (26) Baudrier-Raybaut, M.; Haidar, R.; Kupecek, P.; Lemasson, P.; Rosencher, E. *Nature* **2004**, *432*, 374.

JA903881M